Journal of Organometallic Chemistry 895 (2019) 37–47

Contents lists available at ScienceDirect

Journal of Organometallic Chemistry

journal homepage: www.elsevier.com/locate/jorganchem

Synthesis of ferrocene and azobenzene-based copolymers P(FHEMA-*co*-MAZOHE)s and their redox and photo-responsive properties

Amin Khan [a], Haojie Yu [a, **], Li Wang [a, *], Pavel A. Zhizhko [b], Dmitry N. Zarubin [b], Dmitry A. Lemenovskiy [c], Fazal Haq [a], Muhammad Usman [a], Ahsan Nazir [a], Kaleem-ur-Rehman Naveed [a]

[a] State Key Laboratory of Chemical Engineering, College of Chemical and Biological Engineering, Zhejiang University, Hangzhou, 310027, PR China
[b] A. N. Nesmeyanov Institute of Organoelement Compounds, Russian Academy of Sciences, Vavilov str., 28, 119991, Moscow, Russia
[c] Department of Chemistry, Moscow State University, Vorob'evy Gory 1, 119992, Moscow, Russia

ARTICLE INFO

Article history:
Received 7 March 2019
Received in revised form
29 April 2019
Accepted 13 May 2019
Available online 28 May 2019

Keywords:
Ferrocene
Azobenzene
Materials
Information storage

ABSTRACT

Herein, poly(2-(methacryloyloxy) ethyl ferrocene carboxylate-*co*-(methacrylohydroxyhexane azobenzene)s) (P(FHEMA-*co*-MAZOHE)s) were prepared by random copolymerization and were characterized by proton nuclear magnetic resonance (^{1}H NMR) and gel permeation chromatography (GPC) to confirm the structures and molecular weights respectively. Thermal variations were analyzed by thermogravimetric (TG), differential thermogravimetric (DTG) and differential scanning calorimetry (DSC) techniques. Finally, redox and photo stimuli-responsive properties were confirmed by cyclic voltammetry (CV) and ultraviolet–visible spectroscopy (UV–vis) respectively. The results revealed that (P(FHEMA-*co*-MAZOHE)s) can be useful as information storage materials.

1. Introduction

Information storage materials are playing an increasingly important role in our daily life [1] and in both industrial and academic communities [2,3]. Among different storage materials, redox and photoresponsive polymeric materials are the promising candidates for this purpose. These materials can provide better properties in terms of their rapid, clean and efficient response [4–6]. It is expected that the organometallic complexes containing photo-responsive moieties can serve well as information storage materials due to the synergistic characteristics obtained from the incorporation of redox-responsive moieties into the polymeric system [7–9].

Among different organometallic moieties, ferrocene-based polymers have emerged as a significant class of materials due to the unique properties and structure of ferrocene constituent [10–12]. The explosive studies of ferrocene-containing polymers had started due to their distinctive features such as better redox activity, high chemical and thermal stability and easy solution processability [13]. All these attributes made ferrocene an attractive part of the scientific endeavor [14,15]. In the past decade, several ferrocenes containing systems have been synthesized and extensively explored in different applications such as information storage [16,17] and so on [18–26]. Meng et al. and Xiang et al. paved a way towards the ferrocene-based charge storage materials for organic battery application. The obtained results showed that these materials were good candidates of storage materials due to the better redox reversibility and excellent charge/discharge performance [27,28]. It was expected that these materials can be used for redox-responsive storage devices. In another work, Jin and coworkers synthesized ferrocene-based nonvolatile memory devices in which ferrocene was covalently bonded to reduced graphene oxide [29]. Among available photoactive systems, azobenzene-based polymers have attracted the scientific community due to their versatile properties [30]. Several important applications such as information storage [31,32] and many others [33–36] can be obtained from azobenzene-based systems. Photo-responsive polymers can change their physical and chemical characteristics at a specific wavelength [37,38]. Azobenzene's structure shows light sensitivity due to the reversible *trans*(non-polar)-*cis*(polar) isomerization accompanied by a change in the

* Corresponding author.
** Corresponding author.
E-mail addresses: hjyu@zju.edu.cn (H. Yu), opl_wl@dial.zju.edu.cn (L. Wang).

https://doi.org/10.1016/j.jorganchem.2019.05.009
0022-328X/

dipole moment from 0 D to 3 D [39]. Jiang and co-workers synthesized poly(aryl ether ketone) terminated by azobenzene chromophores. They applied this azobenzene-based system to the surface relief gratings [40] whereas in another Liu and co-workers synthesized azobenzene-based vinyl carbazoles and used them as information storage materials [41]. By combining the properties of ferrocene and azobenzene, four states information storage devices can be prepared. Kurihara et al. synthesized m-ferrocenylazobenzene and reported a unique sequence of properties by using single green light [42]. Similarly, Namiki and co-workers synthesized a few ferrocene and azobenzene-based modified polymeric particles to overcome the instability of the small molecule [43]. However, storage devices which are constructed from small molecules having photo responsive groups usually suffer from less photo mechanical properties [29].

In our previous work, we have designed a system to decrease the photo-oxidation and π-π stacking of the azobenzene chromophore by introducing a methyl group on the electron-rich benzene rings. We also provided with an idea of four states information storage application by employing ferrocene and azobenzene-based polymer in that work [44]. In this work, we have targeted our focus to increase the photo mechanical properties of the azobenzene chromophore which is also an important parameter to address for preparing stable information storage materials. It is expected that by introducing longer alkyl chains with azobenzene can enhance the photo mechanical properties of the polymer [45]. For this purpose, (P(FHEMA-*co*-MAZOHE)s) will be synthesized and their reversible redox and photo responsive properties will be investigated.

2. Experimental section

2.1. Materials

All the organic solvents including dichloromethane (DCM, analytical reagent (AR)), Tetrahydrofuran (THF, AR), triethylamine (Et_3N, AR) and pyridine (AR) were supplied by Sinopharm Chemical Reagent Co. Ltd. Methacrolyl chloride (95%) and hydroxyethyl methacrylate (HEMA, 96%) were purchased from Acros Organics. Azobisisobutyronitrile (AIBN) and ferrocene carboxylic acid (AR) were supplied by Aladdin. *p*-Hydroxyazobenzene (>95%), 1-chloro-6-hyrdoxyhexane and tetrabutylammonium tetrafluroborate (Bu_4NBF_4) were delivered by J & K Scientific Co. Ltd. DCM and Et_3N were dried firstly by activated 4 Å-type molecular sieves and then distilled over calcium hydride while THF was dried firstly by activated 4 Å-type molecular sieves and then distilled over potassium. Pyridine was also dried using activated 4 Å-type molecular sieves. Other chemicals were used without further purification.

2.2. Synthesis of 2-(methacryloyloxy)ethyl ferrocene carboxylate (FHEMA) [46]

Ferrocene carbonyl chloride was synthesized according to the reported literature [46]. Firstly, ferrocene monocarbonyl chloride (6.3219 g, 24.7 mmol) was dissolved in 77.0 mL of THF and then pyridine (1.90 mL, 24.6 mmol) and HEMA (3.20 mL, 26.3 mmol) were added to the previous solution under inert (Ar gas) atmosphere. The reaction was carried on for 5 h and after that, the precipitates were separated from the reaction media by filtration. The obtained filtrate was dried by using rotary evaporator. Finally, the washing was performed using Na_2CO_3 (saturated solution) and deionized water twice (each one) to convert the crude product obtained from rotary evaporation to pure product. The pure product (FHEMA) was retained in a vacuum oven at 40 °C until the complete removal of residual solvents.

2.3. Synthesis of 6-hydroxyhexane azobenzene (AZO6OHE) [47]

p-Hydroxyazobenzene (4.0301 g, 20.0 mmol), potassium carbonate (1.3891 g, 10.0 mmol) and potassium iodide (40.9 mg, 0.24 mmol) were dissolved in 60.0 mL of dry DMF, followed by dropwise addition of 1-chloro-6-hydroxyhexane (4.0 mL, 30.0 mmol). After 10 h reaction at 110 °C, the resulting mixture was precipitated in deionized water. The crude product obtained after filtration was washed by deionized water three times. Then the crude product was dissolved in 250 mL of ethanol and the solution was put into refrigerator to recrystallize in ethanol for two times. The pure product (AZO6OHE) was kept in a vacuum oven at 40 °C until the complete removal of residual solvents.

2.4. Synthesis of methacrylohydroxyhexane azobenzene (MAZOHE) [47]

Firstly, AZO6OHE (1.2611 g, 4.0 mmol) was vacuum dried for 15 min and dissolved in THF (70.0 mL) under an inert atmosphere. After that, TEA (0.7 mL, 5.0 mmol) was added in the previous solution. Methacrolyl chloride (0.5 mL, 5.0 mmol) was added dropwise at 0 °C in the same solution and then the reaction was proceeded at this stage for 2 h and for 10 h at room temperature. Afterward, the precipitates were separated from the reaction media by filtration. The obtained filtrate was dried by using rotary evaporator. Finally, the washing was accomplished using Na_2CO_3 (saturated solution) and deionized water twice (each one) to convert the crude product obtained from rotary evaporation to pure product. The pure product (MAZOHE) was placed in a vacuum oven at 40 °C until the complete removal of residual solvents.

2.5. Synthesis of poly(2-(methacryloyloxy) ethyl ferrocene carboxylate-co-(methacrylo hydroxyhexane azobenzene)) P(FHEMA-co-MAZOHE)

Free radical polymerization was carried out for the copolymerization of FHEMA and MAZOHE [48]. All the copolymers were obtained following the same procedure with the difference in the mole ratios of monomers (FHEMA, MAZOHE). Thereby, the synthesis of P(FHEMA-*co*-MAZOHE)-1 was taken as an illustration. In a typical procedure, FHEMA (0.3431 g, 1.0 mmol), MAZOHE (0.3664 g, 1.0 mmol) and AIBN (0.0032 g, 0.02 mmol) were dissolved in DMF (2.0 mL) and purged with Ar gas for 0.5 h to eradicate the availability of oxygen. After that, the reaction mixture was stirred for 12 h at 90 °C. After completing the reaction, the mixture was added dropwise in methanol (250 mL) to get the precipitates. The precipitates were further purified by repeated dissolution in THF and precipitation in methanol twice. Finally, the resulting solution was centrifuged, filtered and dried in a vacuum oven to obtain a yellowish product.

2.6. Characterization

^1H NMR spectra of the synthesized copolymers were recorded using a Bruker Advanx-600 MHz NMR spectrometer. The weight average molecular mass (M_w) and number average molecular mass (M_n) were determined with waters 1524/2414 as gel permeation chromatography (GPC) instrument. THF was used as a mobile phase and the molecular weight of all the copolymers was calibrated against polymethylmethacrylate (PMMA) standard. Thermal stability and degradation of the polymers were measured using TA-Q500 (Metler-Toledo) with a heating rate of 10 °C/min. The glass transition temperature (T_g) of the polymers were obtained using DSC-Q200 with a heating rate of 10 °C/min. The photoisomerization behavior of the polymers was recorded using a UV/vis Unico

spectrophotometer. The sample solution had a concentration of 0.05 mM for the analysis. The CV curves were recorded on a CHI-630A electro-chemical analyzer (CH Instruments, Inc., Austin, Texas). The concentration of polymers and electrolyte (Bu_4NBF_4) were 0.5 mM and 0.1 M respectively for all the samples. A silver (Ag) electrode was used as a reference electrode while a platinum wire electrode was used as the counter electrode. The working electrode (glassy carbon) was provided with a mirror finish using 0.05 μm Al_2O_3 paste followed by washing under ultrasonication with alcohol/deionized water for 30 s and finally dried at room temperature before use.

3. Results and discussion

3.1. Synthesis and characterization of P(FHEMA-co-MAZOHE)s

FHEMA was obtained by esterification reaction of ferrocene carbonyl chloride and HEMA (Scheme 1a). AZO6OHE was synthesized by the reaction of *p*-hydroxyazobenzene and 1-chloro-6-hydroxyhexane (Scheme 1b). The synthesis of MAZOHE was successfully performed by the reaction of AZO6OHE and methacrolyl chloride (Scheme 1c). Free radical polymerization was executed to synthesize P(FHEMA-*co*-MAZOHE)s using AIBN as an initiator. The synthetic route of P(FHEMA-*co*-MAZOHE) has been given in Scheme 1(d). Table 1 explains the synthetic details of the co-polymers (P(FHEMA-*co*-MAZOHE)s) while Table 2 illustrates the obtained mole ratios and molecular weights of the copolymers. The structures of FHEMA, AZO6OHE and MAZOHE were confirmed by ^{1}H NMR as shown in Fig. 1 (a, b and c) respectively (see Scheme 2).

The obtained chemical shifts for FHEMA were as follows: δ (ppm) = 6.07 (1H, H_a), 5.71 (1H, H_b), 4.72 (2H, H_c), 4.48 (2H, H_d), 4.39 (4H, H_e, H_f), 4.19 (5H, H_g), 1.89 (3H, H_h).

The obtained characteristic chemical shifts for AZO6OHE were as follows: δ (ppm) = 7.87–7.94 (4H, H_a), 7.47–7.50 (2H, H_b), 7.41–7.44 (1H, H_c), 6.98–7.00 (2H, H_d), 4.03–4.05 (2H, H_e), 3.65–3.67 (2H, H_f), 1.43–1.86 (8H, H_g).

Following characteristic peak shifts were found for MAZOHE: δ (ppm) = 7.87–7.92 (4H, H_a), 7.47–7.50 (2H, H_b), 7.41–7.43 (1H, H_c), 6.98–6.99 (2H, H_d), 6.09 (1H, H_e), 5.54 (1H, H_f), 4.14–4.17 (2H, H_g), 4.03–4.05 (2H, H_h), 1.93 (3H, H_i), 1.44–1.83 (8H, H_j).

The peaks area between 6.75-8.0 ppm and 4.0–5.0 ppm belong to azobenzene and ferrocene respectively as explained in ^{1}H NMR spectra (Fig. 1).

Due to the conjugate structure of MAZOHE which can cause space resistance in copolymerization, the ratio of FHEMA was kept higher than 1. Three different copolymers *i.e.* P(FHEMA-*co*-MAZOHE)-1, P(FHEMA-*co*-MAZOHE)-2 and P(FHEMA-*co*-MAZOHE)-3 were obtained in a result. The characteristic peaks of the synthesized copolymers (P(FHEMA-*co*-MAZOHE)s) were confirmed by ^{1}H NMR spectra as shown in Fig. 2 whereas the disappearance of a double bond containing a characteristic peak shift between 5.5 and 6.5 ppm indicated that the unreacted

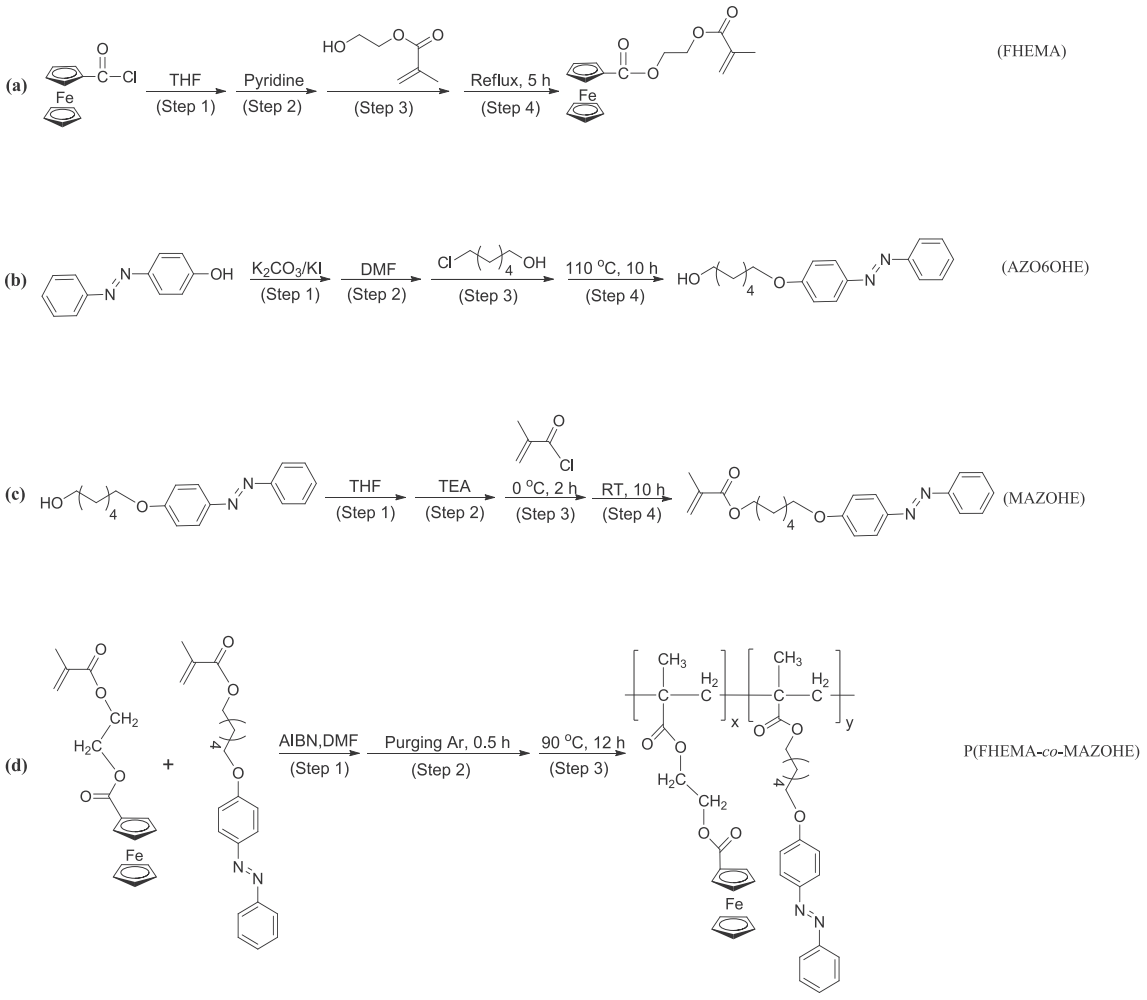

Scheme 1. Synthetic routes for (a) FHEMA, (b) AZO6OHE, (c) MAZOHE and (d) P(FHEMA-*co*-MAZOHE).

Table 1
Synthetic details of P(FHEMA-co-MAZOHE)s.

Sample	Step 1								Step 2	Step 3	
	FHEMA (A)		MAZOHE (B)		AIBN (C)		Mole ratio	DMF	Ar purging	T	t
	g	mmol	g	mmol	g	mmol	A:B:C	mL	h	oC	h
P(FHEMA-*co*-MAZOHE)-1	0.3431	1.00	0.3664	1.00	0.0032	0.02	1:1:0.02	2.0	0.5	90	12
P(FHEMA-*co*-MAZOHE)-2	0.6865	2.00	0.3664	1.00	0.0049	0.03	2:1:0.03	2.5	0.5	90	12
P(FHEMA-*co*-MAZOHE)-3	1.0291	3.00	0.3664	1.00	0.0065	0.04	3:1:0.04	2.5	0.5	90	12

Table 2
GPC results and ratios of each unit.

Sample	P(FHEMA-*co*-MAZOHE)s (GPC			P(FHEMA-*co*-MAZOHE)s (NMR, GPC)		
	Mn	Mw	PDI	(x:y) (NMR	m(FHEMA)n	(MAZOHE)
P(FHEMA-*co*-MAZOHE)-1	8126	22715	2.79	0.97:1	5.7	5.6
P(FHEMA-*co*-MAZOHE)-2	6016	19952	3.31	1.98:1	5.6	2.8
P(FHEMA-*co*-MAZOHE)-3	6824	38667	5.66	2.95:1	7.1	2.4

While, m: number of repeating units for FHEMA and n: number of repeating units for MAZOHE.

monomers were completely removed.

Fig. 3A explains the GPC curves of the synthesized copolymers. The polydispersity index of the copolymers found to be high which might be due to the formation of unequal chain lengths in the final obtained copolymers. It can also be observed that the value of polydispersity index (PDI) is increasing by increasing the amount of FHEMA. Basically, ferrocene moiety plays the role of radical scavenger in the copolymerization systems which is also well explained by Noriyuki and co-workers [49]. Due to the radical scavenging ability of ferrocene the chances of retardation in copolymerization system increases. As the amount of FHEMA is increasing so the retardation rate is also increasing. This retardation amplifies the formation of chains in different lengths which in turn increases the PDI in the polymerization systems [49].

Following characteristic peak shifts were found for P(FHEMA-*co*-MAZOHE)-1: δ (ppm) = 7.85 (4H, H_a, H_b), 7.43 (3H, H_c, H_d), 6.93 (2H, H_e), 4.80 (2H, H_f), 4.37 (6H, H_g, H_h, H_i), 4.17 (5H, H_j), 3.92 (4H, H_k, H_l), 1.24–1.86 (12H, H_m, H_n), 0.89–1.11 (6H, H_o).

Following characteristic peak shifts were found for P(FHEMA-*co*-MAZOHE)-2: δ (ppm) = 7.86 (4H, H_a, H_b), 7.46 (3H, H_c, H_d), 6.96 (2H, H_e), 4.80 (4H, H_f), 4.38 (12H, H_g, H_h, H_i), 4.18 (10H, H_j), 3.95 (4H, H_k, H_l), 1.25–1.87 (14H, H_m, H_n), 0.90–1.18 (9H, H_o).

Following characteristic peak shifts were found for P(FHEMA-*co*-MAZOHE)-3: δ (ppm) = 7.90 (4H, H_a, H_b), 7.48 (3H, H_c, H_d), 6.99 (2H, H_e), 4.82 (6H, H_f), 4.41 (18H, H_g, H_h, H_i), 4.18 (15H, H_j), 3.97 (4H, H_k, H_l), 1.26–1.87 (16H, H_m, H_n), 0.88–1.17 (12H, H_o).

The TGA curves (Fig. 3B) showed that the degradation of the polymers was a multistage process. The initial decomposition temperature of all the three copolymers attributed to the breakage of the azo group[32]. The stability of the azo group might be enhanced due to the longer alkyl chain attached with it. This initial putrefaction of P(FHEMA-*co*-MAZOHE)-1, P(FHEMA-*co*-MAZOHE)-2 and P(FHEMA-*co*-MAZOHE)-3 appeared at 309 °C, 271 °C and 289 °C respectively. After that, the ester bonds (C=O and C–O), connected with the ferrocene moieties, were broken producing a big amount of carbon dioxide, which is responsible for the second stage of weight loss up to 371 °C, 325 °C and 366 °C for P(FHEMA-*co*-MAZOHE)-1, P(FHEMA-*co*-MAZOHE)-2 and P(FHEMA-*co*-MAZOHE)-3 respectively. Finally, the bonds between Fe–C were broken. This decomposition produced Fe atoms in abundance which possibly fastened the polymer degradation after 550 °C. The similar kind of degradation can be observed from the DTG curves (Fig. 3C). Fig. 3D represents the DSC curves of synthesized copolymers which revealed that T_g of the copolymers depends on the final percentage of ferrocene and azobenzene. (FHEMA-*co*-MAZOHE)-1, P(FHEMA-*co*-MAZOHE)-2 and P(FHEMA-*co*-MAZOHE)-3 depicted T_g of 68 °C, 83 °C and 86 °C respectively.

The T_g of P(FHEMA-*co*-MAZOHE)-3 was found to be higher in comparison with the other two copolymers. This was mainly due to the higher percentage of ferrocene group which enhanced the thermal transition of the synthesized copolymer.

3.2. Photo isomerization properties of P(FHEMA-co-MAZOHE)s

The reversible *trans-cis* isomerization of azobenzenes can be described as a geometrical isomerization. The inter-conversion of *cis-trans* isomers of azobenzene is not visualized as a precise color change, as in the case for most of the other photoactive transformations however the difference between the isomers can be seen based on their specific wavelengths. The photoisomerization changes the size and geometry of the azobenzene at the molecular level. The *trans*-form of azobenzene is more dominant under dark or typical ambient illumination. The *cis* isomers of azobenzene tend to reconvert to their more stable *trans*-form after a certain interval of time depending on the environment and substitution pattern of azobenzene [39,50–52]. The isomerization behavior of azobenzene has been studied broadly by the scientific community but its precise pathway is still vague which requires further clarifications [53–55].

The polymer samples (prepared in DMF) were irradiated with UV light (365 nm) to induce configurational changes in the azobenzene. After the UV irradiation, two characteristic absorption peaks were observed (π-π^* and n-π^*). The π-π^* band was more intense in comparison with the n-π^* band. Upon UV irradiation (365 nm), the absorption peak was decreased at about 346 nm due to the π-π^* electron transition of the *trans*-isomer while the absorption peak at 440 nm was increased slightly due to n-π^* transition of the *cis*-isomer of azobenzene. The isosbestic point was observed at about 410 nm after passing UV irradiation at several intervals of time Fig. 4(a–c). The *trans-cis* behavior of azobenzene was observed when the absorption bands were decreased due to π-π^* electron transition (346 nm) and increased because of the n-π^* transition (440 nm) after the UV light irradiation. The electronic n-π^* transition is only allowed in *cis* isomers, and the characteristic band at 440 nm is indicative of the formation of the *cis* isomer upon UV irradiation.

After that, the visible light was irradiated at the samples at different elongations of time and their reversible *cis-trans* behavior

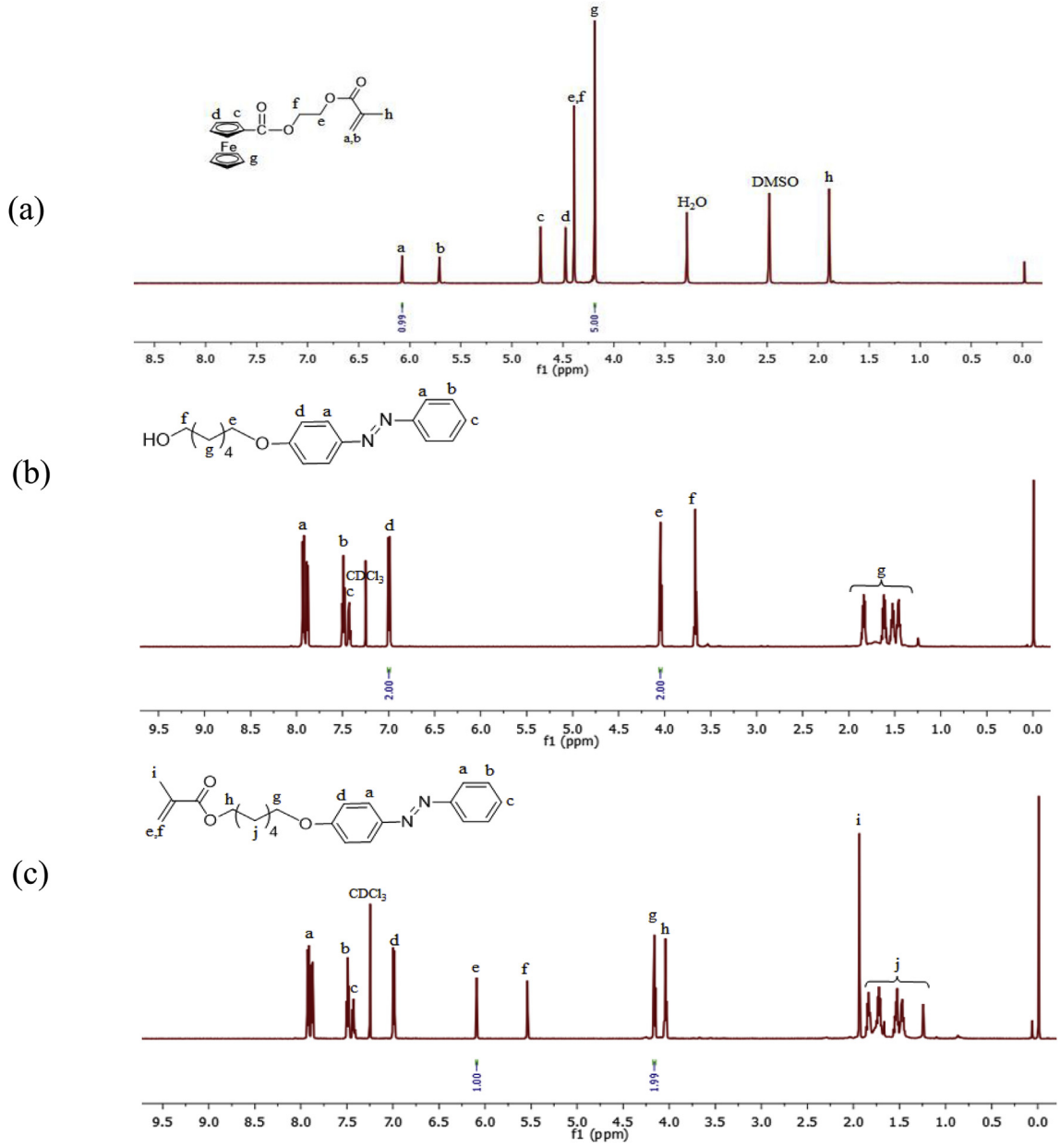

Fig. 1. ^{1}H NMR spectra of (a) FHEMA, (b) AZO6OHE and (c) MAZOHE.

was observed. The *cis*-isomer of azobenzene started restoring back to their *trans*-form after the visible light irradiation Fig. 4 (a'-c'). This *trans*-to-*cis* and *cis*-to-*trans* behavior of the polymers indicated that these copolymers are good candidates for photoisomerization. These results can also be attributed to the photomechanical properties as reported by Luigi and co-workers [56]. According to Luigi et al., by using first class (azobenzene-type) of azo-chromophore and by increasing volume variation (occurs usually due to the longer alkyl chain) can enhance the photomechanical properties. In present study, the azobenzene chromophore is of the first class (azobenzene-type) carrying longer alkyl chain, according to Rau classification scheme [57]. The other two classes, the amino and pseudo-stilbene types, as described by Rau, are characterized on the contrary by overlapping bands, which allow only a resonant

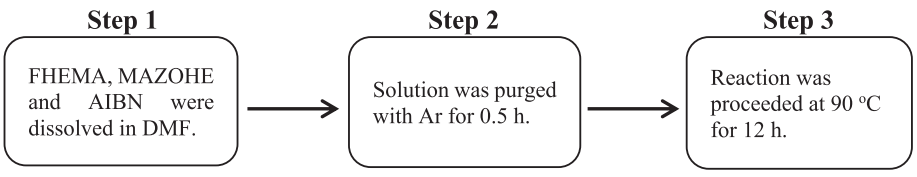

Scheme 2. Stepwise procedure for the synthesis of P(FHEMA-*co*-MAZOHE).

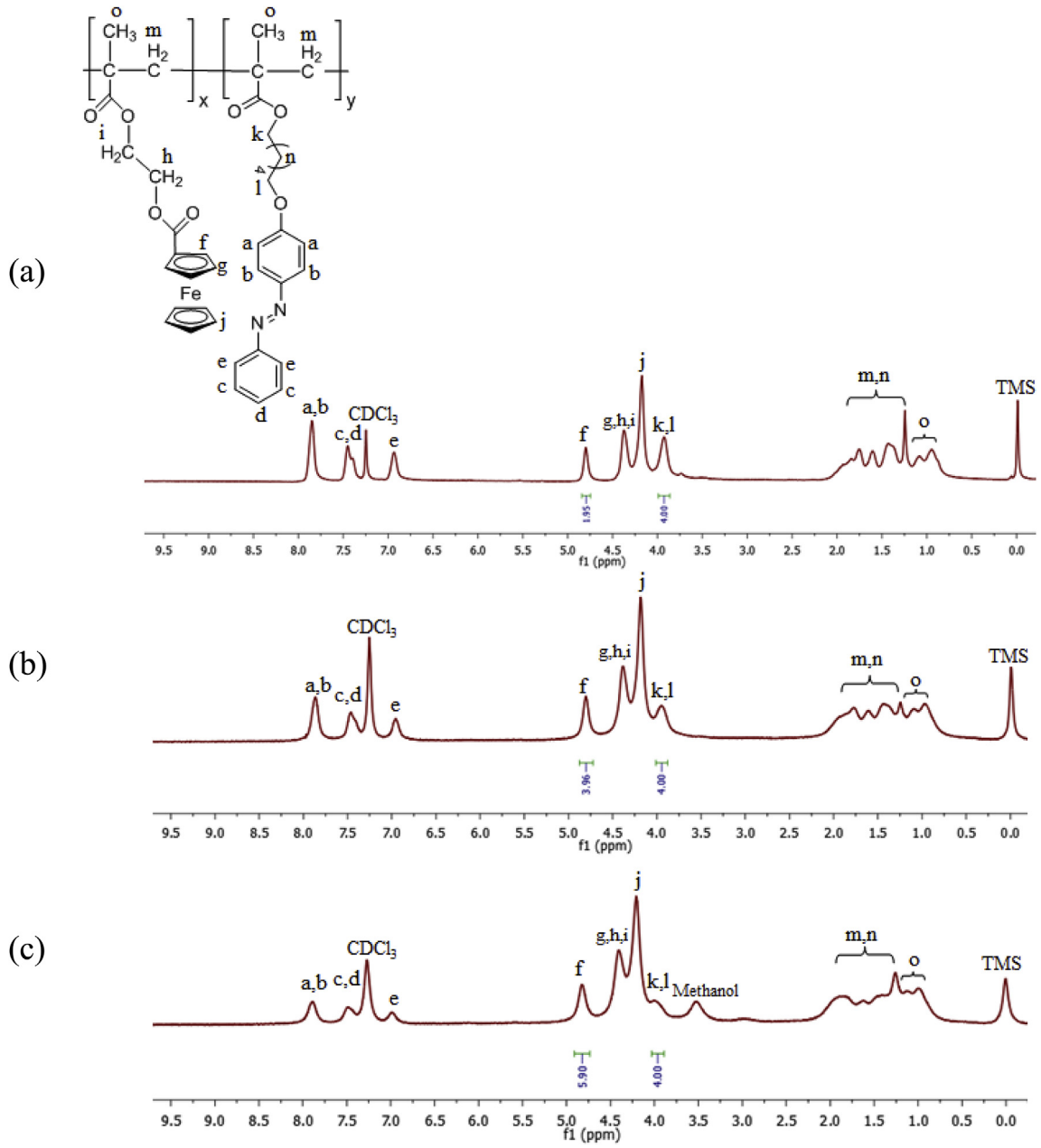

Fig. 2. ^{1}H NMR spectra of (a) P(FHEMA-*co*-MAZOHE)-1, (b) P(FHEMA-*co*-MAZOHE)-2 and (c) P(FHEMA-*co*-MAZOHE)-3.

photoisomerization and a shorter *cis* isomer lifetime. Both these effects do not permit an efficient *trans*-to-*cis* isomerization, whereas an almost complete conversion is possible with azobenzene-type derivatives. Thus, the possibility of moving the relative isomeric population for a wider range allows to obtain a higher macroscopic volume variation. From Fig. 4, we can see that the P(FHEMA-*co*-MAZOHE)s provided almost reversible conversion which can be correlated with the photomechanical enhancement [56]. So, it can be concluded that the synthesized polymers affected the photomechanical properties in a constructive way.

3.3. Electrochemical properties of P(FHEMA-co-MAZOHE)s

The electrochemical process involves loss and gain of electrons. The electrochemical properties of ferrocene-based polymers are important to investigate their potential application as an information storage material. CV is considered as one of the suitable methods to determine electrochemical properties among different available methods [58]. The electrochemical properties of the polymers (0.5 mM) were studied in DCM, DMSO, DMF and THF containing Bu_4NBF_4 (0.1 M) as a supporting electrolyte at room temperature. The results indicated that the scan rates and solvent polarity had drastic effects on the CV curves [59,60]. The electrochemical properties of the synthesized copolymers were affected by the potential scan rates and a variety of solvents. CV curves of P(FHEMA-*co*-MAZOHE)-1, P(FHEMA-*co*-MAZOHE)-2 and P(FHEMA-*co*-MAZOHE)-3 were affected by the solvent due to the change in the polarity of the solvent. The increase in polarity of the solvent resulted in the deformation of the shape of the peak. The shape of the peaks was found compact and deformed in high polar solvents like DMF and DMSO whereas both reduction and oxidation peaks potential were decreased with the increase in solvent

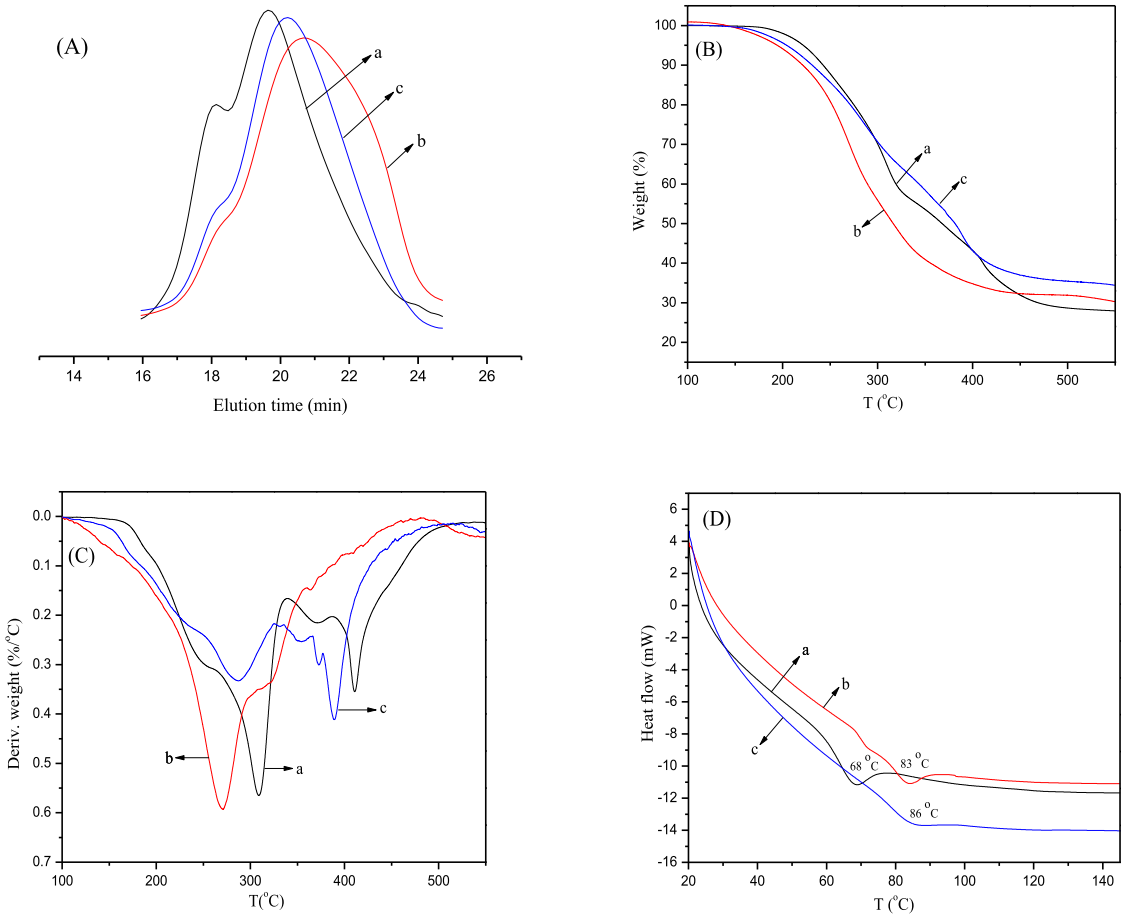

Fig. 3. (A) GPC curves of (a) P(FHEMA-*co*-MAZOHE)-1, (b) P(FHEMA-*co*-MAZOHE)-2 and (c) P(FHEMA-*co*-MAZOHE)-3; (B) TGA curves of (a) P(FHEMA-*co*-MAZOHE)-1, (b) P(FHEMA-*co*-MAZOHE)-2 and (c) P(FHEMA-*co*-MAZOHE)-3; (C) DTG curves of (a) P(FHEMA-*co*-MAZOHE)-1, (b) P(FHEMA-*co*-MAZOHE)-2 and (c) P(FHEMA-*co*- MAZOHE)-3 and (D) DSC curves of (a) P(FHEMA-*co*-MAZOHE)-1, (b) P(FHEMA-*co*-MAZOHE)-2 and (c) P(FHEMA-*co*-MAZOHE)-3.

polarity as shown in Figs. 5–7.

The most well-defined and sharp peaks were obtained in DCM solution with high current. The lowest peak-to-peak potential separation (ΔEp) was obtained in the solution containing DCM. In CV theory, ΔEp is termed as the peak-to-peak potential separation which is an important parameter to discuss as it explains about the reversibility and irreversibility of the electrochemical process. If peak-to-peak potential separation is high, it means that the process is irreversible and vice versa [56]. The data showed that the diffusion rate of charge was faster and resistance of the solution was smaller in DCM, which showed that redox reactions were more favorable in DCM as compared to the other solvents.

Additionally, it was observed that all the ferrocene units behaved equally in DCM which can also be seen from the appearance of one redox peak in DCM solution while the ferrocene in its oxidized form was more rigid/stable and was hard to reduce in the high polar solvents such as DMSO and DMF. The synthesized polymers also showed sensitivity toward potential scan rate. Peak current values at the cathode (I_{PC}) and anode (I_{PA}) were increased with the increase in potential scan rate which was in accordance with the Fick's law at room temperature [61]. These results showed that reversible electroactive process can be obtained from these polymers.

For a better understanding of redox/photoresponsive based multi-states information storage, a schematic view has been shown in Fig. 8. In the first step, UV light incidents and *trans* azobenzene changes to *cis* azobenzene which can be regarded as state 2 ((a) storage of optical information). In the third state, electrical information is stored, when ferrocene changes to ferrocenium ion ((b) storage of electrical information). The fourth state corresponds with *cis* to *trans* isomerization of azobenzene after consuming the visible light ((c) storage of optical information) and lastly ferrocenium ion turns into its initial state after retrieving the electrical information ((d) storage of electrical information).

4. Conclusion

In the present work, we investigated the information storage behavior of ferrocene and azobenzene-based random copolymers. For this reason, three different copolymers named as P(FHEMA-*co*-MAZOHE)-1, P(FHEMA-*co*-MAZOHE)-2 and P(FHEMA-*co*-MAZOHE)-3 were prepared and characterized by ^{1}H NMR spectra and GPC results. Thermal analysis was performed by TG/DTG analysis. CV curves and UV/vis spectra showed that these copolymers contain good redox and photoresponsive properties respectively. The results also indicated that the polymers can sustain to different intervals of UV–vis light irradiation and also can exhibit redox reaction. All these characteristics showed that when these moieties were combined together, they provided very beneficial redox/photoresponsive behavior and can be used as information storage materials.

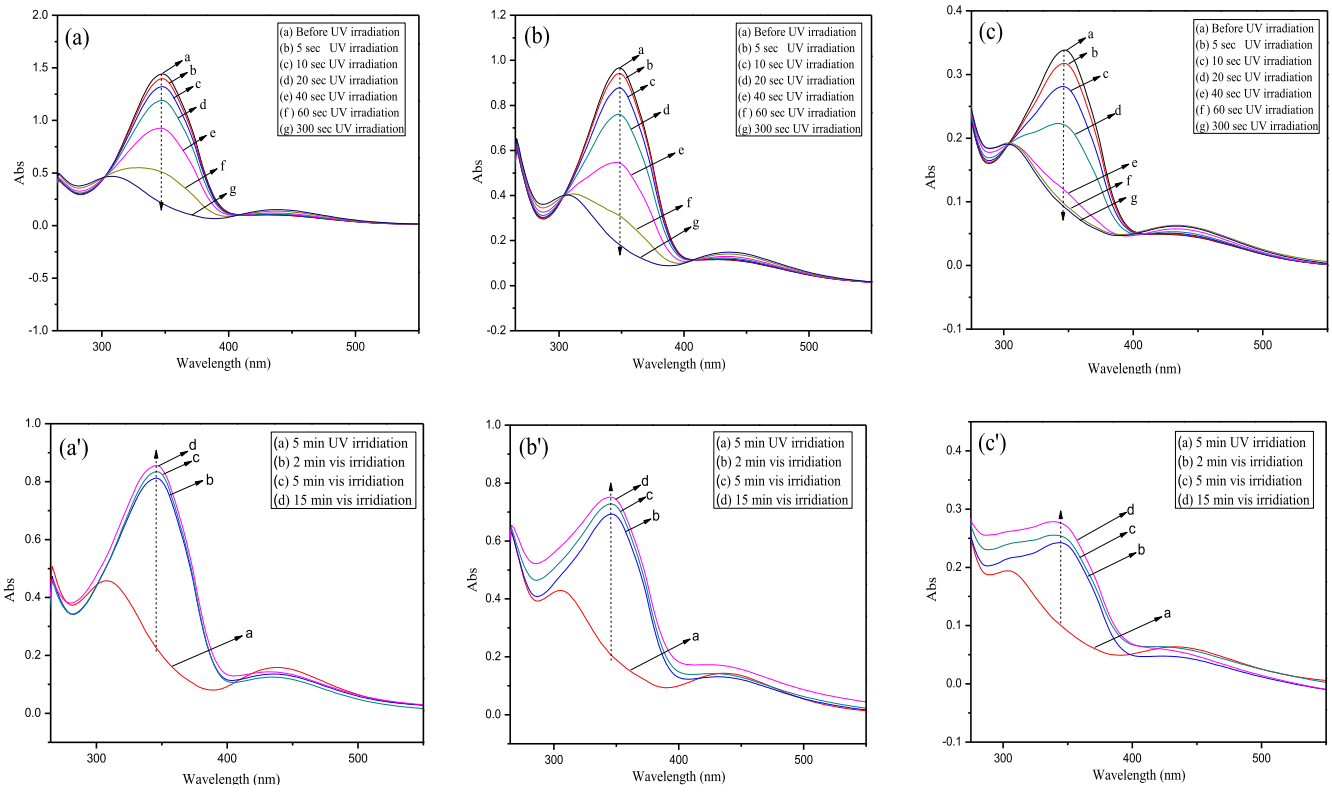

Fig. 4. UV–vis spectra of (a) P(FHEMA-*co*-MAZOHE)-1, (b) P(FHEMA-*co*-MAZOHE)-2 and (c) P(FHEMA-*co*-MAZOHE)-3 at different time intervals of UV light; UV–vis spectra of (a') P(FHEMA-*co*-MAZOHE)-1, (b') P(FHEMA-*co*-MAZOHE)-2 and (c') P(FHEMA-*co*-MAZOHE)-3 at different time intervals of UV and visible light irradiation.

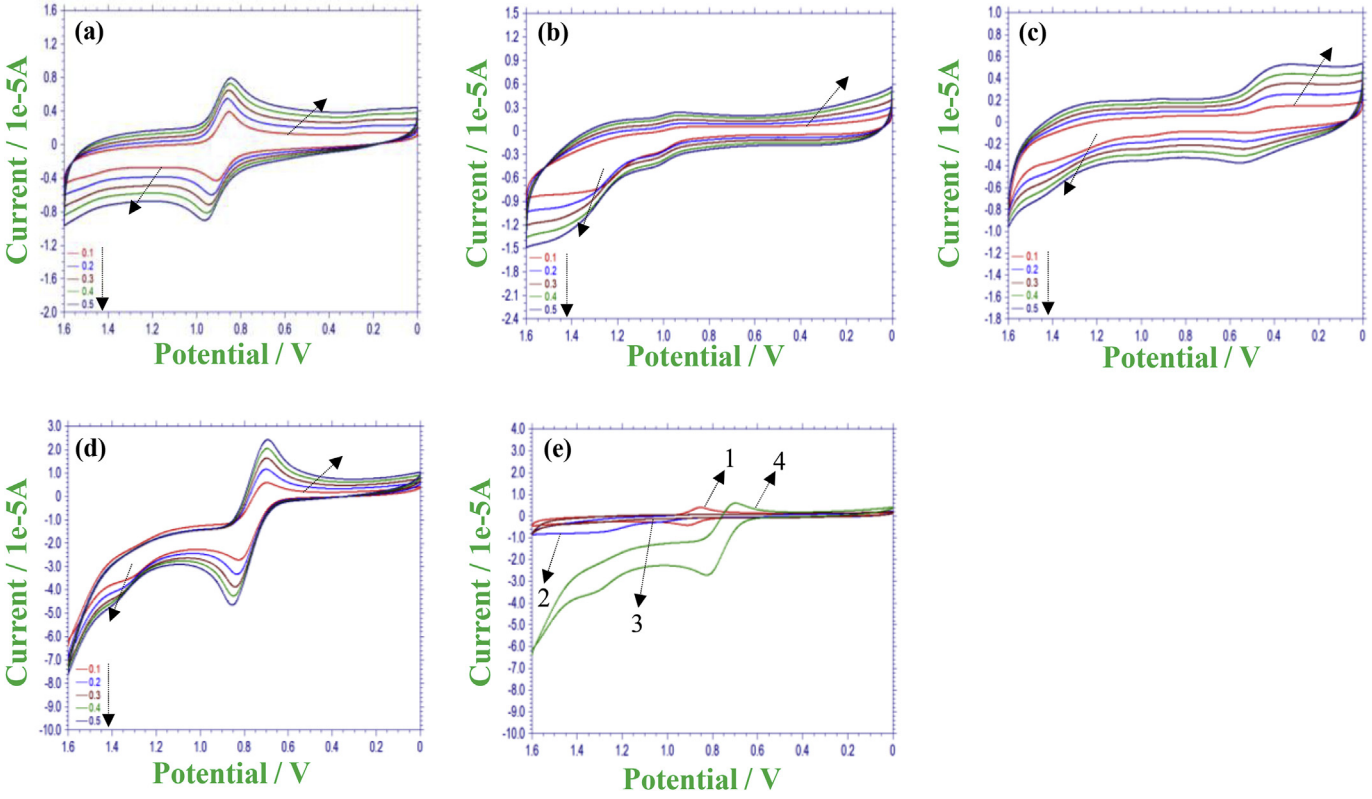

Fig. 5. CV curves of P(FHEMA-*co*-MAZOHE)-1 in (a) DCM, (b) DMF, (c) DMSO and (d) THF at different potential scan rates (direction of arrows means the increase of peaks in terms of current (oxidation and reduction) by increasing the scan rate) and (e) different organic solvents: (1) DCM, (2) DMF, (3) DMSO and (4) THF at 0.1 V/s.

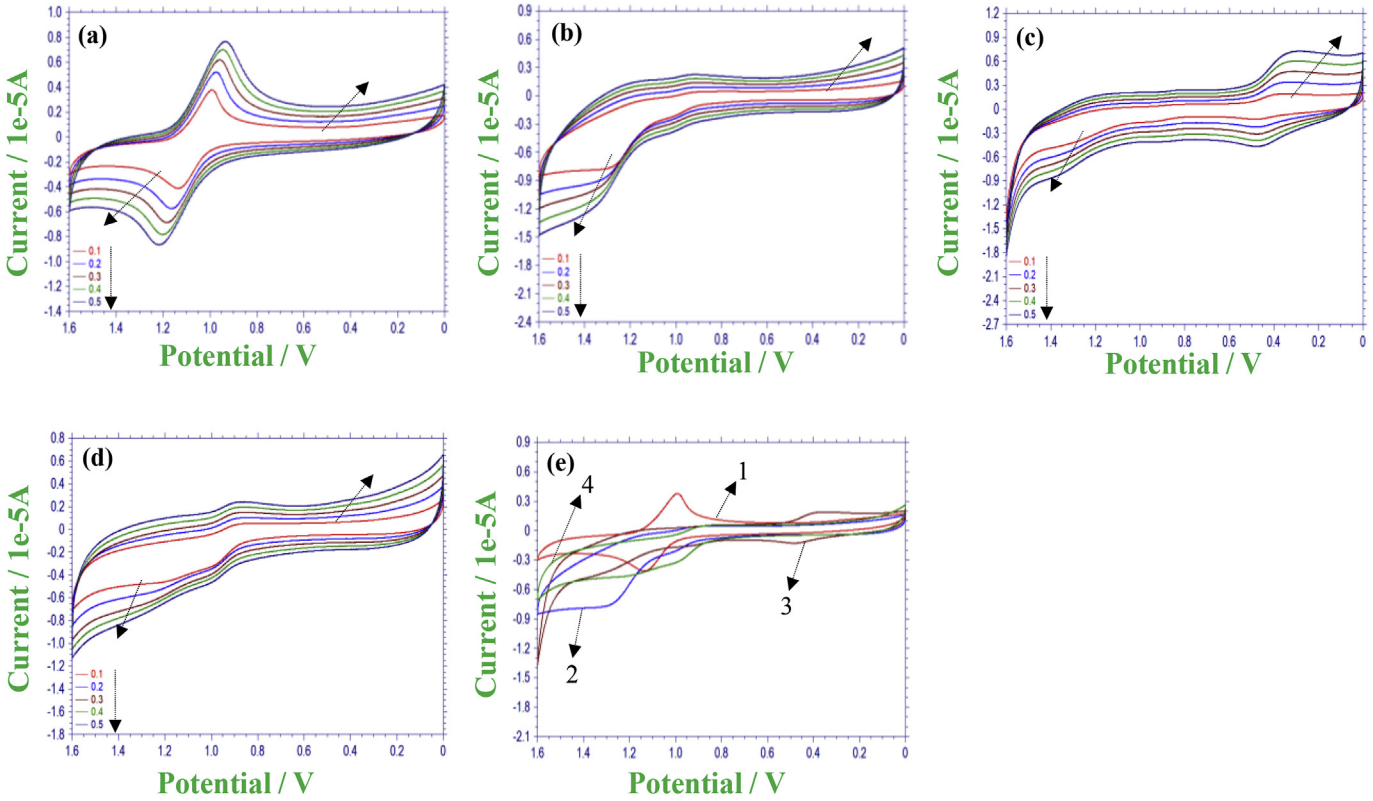

Fig. 6. CV curves of P(FHEMA-*co*-MAZOHE)-2 in (a) DCM, (b) DMF, (c) DMSO and (d) THF at different potential scan rates (direction of arrows means the increase of peaks in terms of current (oxidation and reduction) by increasing the scan rate) and (e) different organic solvents: (1) DCM, (2) DMF, (3) DMSO and (4) THF at 0.1 V/s.

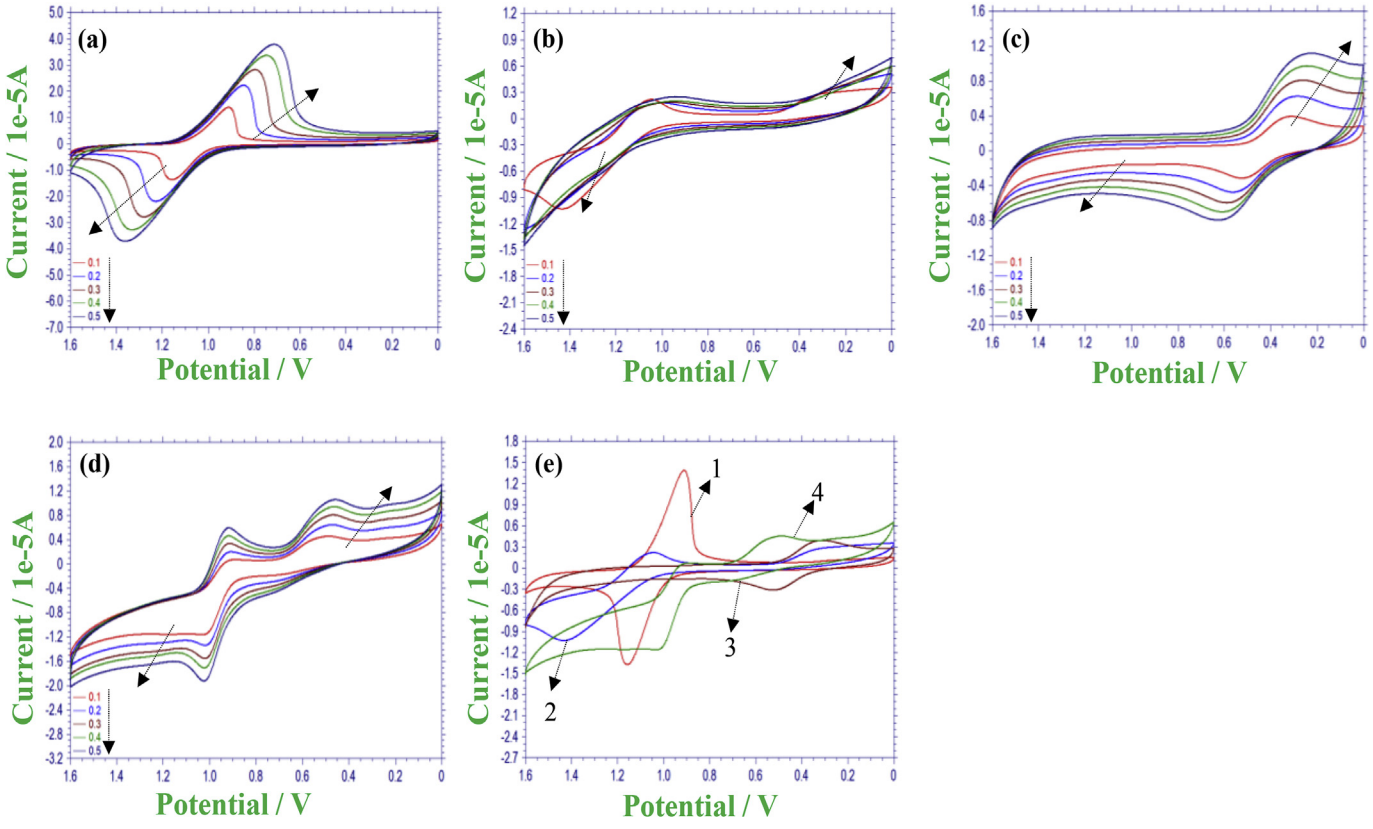

Fig. 7. CV curves of P(FHEMA-*co*-MAZOHE)-3 in (a) DCM, (b) DMF, (c) DMSO and (d) THF at different potential scan rates (direction of arrows means the increase of peaks in terms of current (oxidation and reduction) by increasing the scan rate) and (e) different organic solvents: (1) DCM, (2) DMF, (3) DMSO and (4) THF at 0.1 V/s.

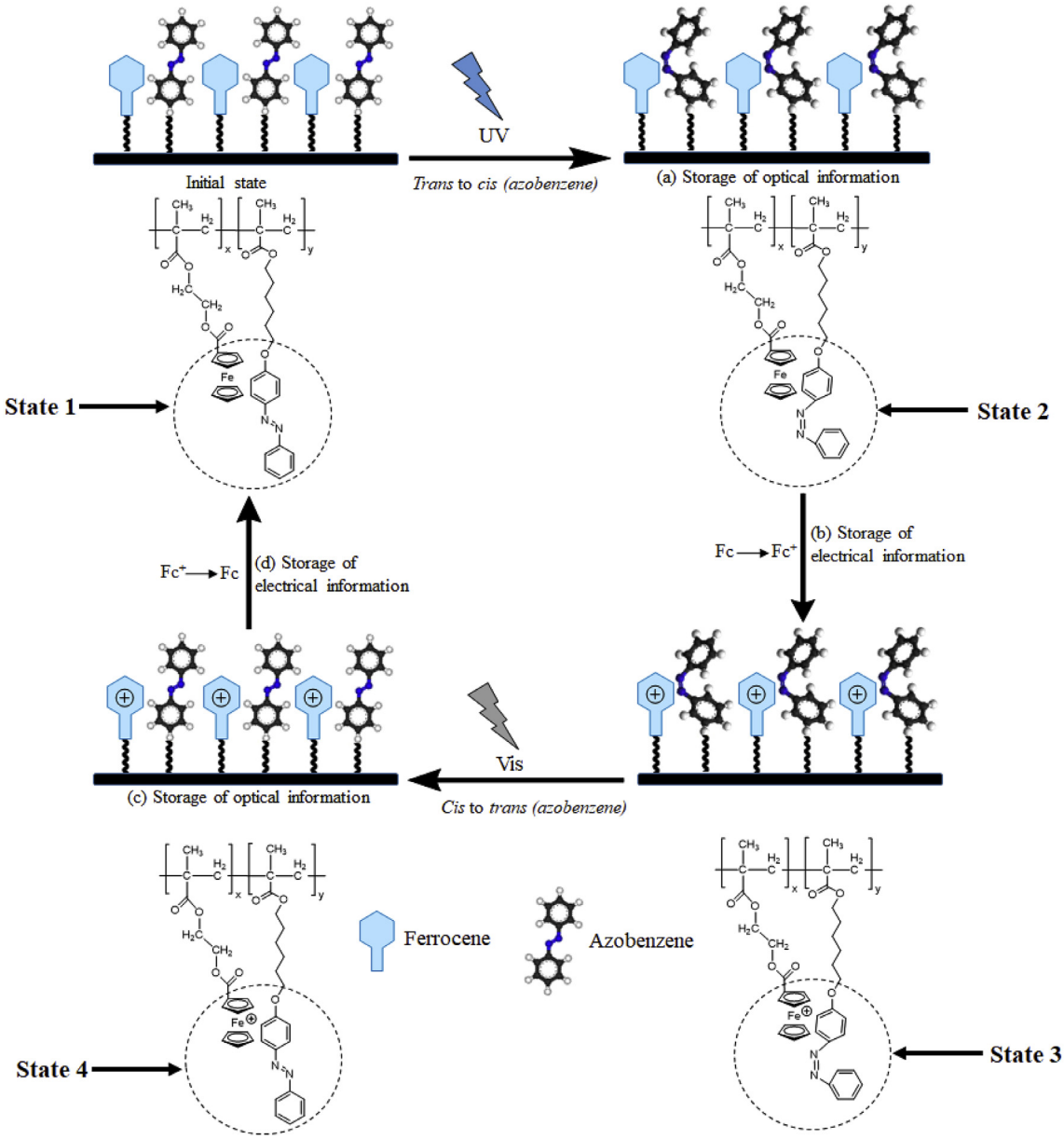

Fig. 8. Schematic model of the multi-states information storage.

Acknowledgment

Financial support from the National Natural Science Foundation of China (51673170, 21472168, 21372200 and 21611530689), the Science and Technology Innovation Team of Ningbo (2011B82002), the Fundamental Research Funds for the Central Universities (2017FZA4023) are gratefully acknowledged.

References

[1] J. Ouyang, Y. Yang, Appl. Phys. Lett. 96 (2010) 063506–063509.
[2] G.W. Burr, B.N. Kurdi, J.C. Scott, C.H. Lam, K. Gopalakrishnan, R.S. Shenoy, IBM J. Res. Dev. 52 (2008) 449–464.
[3] J.C. Scott, L.D. Bozano, Adv. Mater. 19 (2007) 1452–1463.
[4] K. Zhang, J. Liu, Y. Guo, Y. Li, X. Ma, Z. Lei, Mater. Sci. Eng. C 87 (2018) 1–9.
[5] H. Guo, J. Yang, J. Zhou, L. Zeng, L. Zhao, B. Xu, Dyes Pigments 149 (2018) 626–632.
[6] F.S. Pick, D.B. Leznoff, M.D. Fryzuk, Dalton Trans. 47 (2018) 10925–10931.
[7] R. Deschenaux, I. Jauslin, A. Ulrich Scholten, F. Turpin, D.G., B. Heinrich, Macromolecules 31 (2017) 5647–5654.
[8] R.D., F. Turpin, D. Guillon, Macromolecules 30 (2017) 3759–3765.
[9] M.A. Hussein, A.M. Asiri, Des. Monomers Polym. 15 (2012) 207–251.
[10] Z. She, K. Topping, B. Dong, M.H. Shamsi, H.-B. Kraatz, Chem. Commun. 53 (2017) 2946–2949.
[11] R.H. Palmer, J. Liu, C.-W. Kung, I. Hod, O.K. Farha, J.T. Hupp, Langmuir 34 (2018) 4707–4714.
[12] L.E. Wilson, C. Hassenrück, R.F. Winter, A.J. White, T. Albrecht, N.J. Long, Angew. Chem. Int. Ed. 56 (2017) 6838–6842.
[13] R. Gracia, D. Mecerreyes, Polym. Chem. 4 (2013) 2206–2214.
[14] T. Morikita, T. Yamamoto, J. Organomet. Chem. 637 (2001) 809–812.
[15] K. Fujiwara, H. Akutsu, J.I. Yamada, M. Satoh, S.I. Nakatsuji, Tetrahedron Lett. 52 (2011) 6655–6658.
[16] J. Xiang, T.-K. Wang, Q. Zhao, W. Huang, C.-L. Ho, W.-Y. Wong, J. Mater. Chem. C 4 (2016) 921–928.
[17] J. Xiang, X. Li, Y. Ma, Q. Zhao, C.-L. Ho, W.-Y. Wong, J. Mater. Chem. C 6 (2018) 11348–11355.
[18] W.A. Amer, L. Wang, A.M. Amin, L. Ma, H. Yu, J. Inorg, Organomet. Polymer Mater. 20 (2010) 605–615.
[19] R. Tong, Y. Zhao, L. Wang, H. Yu, F. Ren, M. Saleem, W.A. Amer, J. Organomet. Chem. 755 (2014) 16–32.
[20] J. Huo, L. Wang, T. Chen, L. Deng, H. Yu, Q. Tan, Des. Monomers Polym. 10 (2007) 389–404.
[21] J. Xiang, R. Burges, B. Häupler, A. Wild, U.S. Schubert, C.L. Ho, W.Y. Wong,

Polymer 68 (2015) 328–334.
[22] C. Su, Y. Ye, L. Xu, C. Zhang, J. Mater. Chem. 22 (2012) 22658–22662.
[23] H. Zhong, G. Wang, Z. Song, X. Li, H. Tang, Y. Zhou, H. Zhan, Chem. Commun. 50 (2014) 6768–6770.
[24] C. Su, L. Wang, L. Xu, C. Zhang, Electrochim. Acta 104 (2013) 302–307.
[25] U. Muhammad, W. Li, Y. Haojie, H. Fazal, H. Muhammad, S.U. Raja, K. Amin, F. Shah, N. Ahsan, E. Tarig, J. Organomet. Chem. 872 (2018) 40–53.
[26] A. Khan, L. Wang, H. Yu, M. Haroon, R.S. Ullah, A. Nazir, T. Elshaarani, M. Usman, S. Fahad, F. Haq, Appl. Organomet. Chem. 32 (2018) 1–28.
[27] Z. Meng, K. Sato, T. Sukegawa, K. Oyaizu, C.-L. Ho, J. Xiang, Y.-H. Feng, Y.H. Lo, H. Nishide, W.-Y. Wong, J. Organomet. Chem. 812 (2016) 51–55.
[28] J. Xiang, K. Sato, H. Tokue, K. Oyaizu, C.L. Ho, H. Nishide, W.Y. Wong, M. Wei, Eur. J. Inorg. Chem. 2016 (2016) 1030–1035.
[29] C. Jin, J. Lee, E. Lee, E. Hwang, H. Lee, Chem. Commun. 48 (2012) 4235–4237.
[30] A.M. Rosales, C.B. Rodell, M.H. Chen, M.G. Morrow, K.S. Anseth, J.A. Burdick, Bioconjug. Chem. 29 (2018) 905–913.
[31] E. Zarins, K. Balodis, A. Ruduss, V. Kokars, A. Ozols, P. Augustovs, D. Saharovs, Opt. Mater. 79 (2018) 45–52.
[32] D. Gindre, A. Boeglin, A. Fort, L.C. Mager, K.D. Dorkenoo, Optic Express 14 (2006) 9896–9901.
[33] X.L. Jiang, L. Li, J. Kumar, D.Y. Kim, Appl. Phys. Lett. 68 (1996) 2618–2620.
[34] H. Li, C. Wang, Y. Pan, Y. Yang, R. Xia, Optic Commun. 419 (2018) 71–74.
[35] V. Toshchevikov, J. Ilnytskyi, M. Saphiannikova, J. Phys. Chem. Lett. 8 (2017) 1094–1097.
[36] C. Fedele, P.A. Netti, S. Cavalli, Biomater. Sci. 6 (2018) 990–995.
[37] H.M. Bandara, S.C. Burdette, Chem. Soc. Rev. 41 (2012) 1809–1825.
[38] H. Zhou, C. Xue, P. Weis, Y. Suzuki, S. Huang, K. Koynov, G.K. Auernhammer, R. Berger, H.-J. Butt, S. Wu, Nat. Chem. 9 (2017) 145–151.
[39] F. Ercole, Polym. Chem. 1 (2010) 37–54.
[40] X. Jiang, H. Wang, X. Chen, X. Li, L. Lei, J. Mu, G. Wang, S. Zhang, React. Funct. Polym. 70 (2010) 699–705.
[41] G. Liu, B. Zhang, Y. Chen, C.X. Zhu, L. Zeng, D. Siuhungchan, K.G. Neoh, J. Chen, E.T. Kang, J. Mater. Chem. 21 (2011) 6027–6033.
[42] M. Kurihara, A. Hirooka, S. Kume, M. Sugimoto, H. Nishihara, J. Am. Chem. Soc. 124 (2002) 8800–8801.
[43] K. Namiki, M. Murata, S. Kume, H. Nishihara, New J. Chem. 35 (2011) 2146–2152.
[44] A. Khan, L. Wang, H. Yu, M. Haroon, R.S. Ullah, A. Nazir, T. Elshaarani, M. Usman, S. Fahad, K.-u.-R. Naveed, J. Organomet. Chem. 880 (2018) 124–133.
[45] Y. Yue, Y. Norikane, R. Azumi, E. Koyama, Nat. Commun. 9 (2018) 1–8.
[46] M. Saleem, L. Wang, H. Yu, Zain-ul-Abdin, M. Akram, R.S. Ullah, Colloid Polym. Sci. 295 (2018) 995–1006.
[47] R. Dong, B. Zhu, Y. Zhou, D. Yan, X. Zhu, Angew. Chem. Int. Ed. 51 (2012) 11633–11637.
[48] P. Weis, D. Wang, S. Wu, Macromolecules 49 (2016) 6368–6373.
[49] N. Kuramoto, Y. Shishido, K. Nagai, J. Polym. Sci., Polym. Chem. Ed. 35 (1997) 1967–1972.
[50] C. Barrett, A. Natansohn, P. Rochon, Macromolecules 27 (1994) 4781–4786.
[51] C. Barrett, A. Natansohn, P. Rochon, Chem. Mater. 7 (1995) 899–903.
[52] S. Xie, A. Natansohn, P. Rochon, Chem. Mater. 5 (1993) 403–411.
[53] E. Merino, M. Ribagorda, Beilstein J. Org. Chem. 8 (2012) 1071–1090.
[54] G. Tiberio, L. Muccioli, R. Berardi, C. Zannoni, ChemPhysChem 11 (2010) 1018–1028.
[55] C. Dugave, L. Demange, Chem. Rev. 103 (2003) 2475–2532.
[56] L. Angiolini, T. Benelli, L. Giorgini, F. Paris, E. Salatelli, M.P. Fontana, P. Camorani, Eur. Polym. J. 44 (2008) 3231–3238.
[57] H. Rau, Photochem. Photophys. 2 (1990) 119–141.
[58] M. Liang, W. Li, Q. Tan, H. Yu, H. Jia, Z. Ma, H. Hu, Z. Chen, Electrochim. Acta 54 (2009) 5413–5420.
[59] Q. Tan, L. Wang, L. Ma, H. Yu, Q. Liu, A. Xiao, Macromolecules 42 (2009) 4500–4510.
[60] C. Li, L. Wang, L. Deng, H. Yu, J. Huo, L. Ma, J. Wang, J. Phys. Chem. B 113 (2009) 15141–15147.
[61] R. Holze, Angew. Chem. Int. Ed. 114 (2010) 677–680.